NUCLEOSYNTHETIC STRONTIUM ISOTOPE ANOMALIES IN CARBONACEOUS CHONDRITES. T.

Yokoyama[1], H. Yamazaki[1], and S. Hasegawa[1] [1]Department of Earth and Planetary Sciences, Tokyo Institute of Technology, Japan (tetsuya.yoko@geo.titech.ac.jp).

Introduction: The origin of planetary scale isotope heterogeneity in the early Solar System is still controversial. A key observation is that some elements possess isotope anomalies in various meteorites (e.g., Ti, Cr, Sr, Mo, Sm) [1-4], whereas some do not show any resolvable isotope anomalies in the same meteorites (e.g., Te, Hf, Os) [5-7]. The inconsistency would be attributed to a consequence of incomplete mixing of dust grains [8] or destruction of some selected presolar materials via nebular thermal processing [1]. However, the details regarding the processes that may have led to isotope heterogeneity are not totally understood.

To resolving this issue, precise and accurate isotope analysis of multiple elements for various types of meteorites is essential, particularly with special care when analyzing samples containing acid resistant presolar grains. Here, we present a new aggressive acid digestion method for chondrites aimed for achieving complete dissolution of acid-resistant presolar grains (e.g., SiC). The new technique was applied for precise determination of Sr isotope anomalies in three carbonaceous chondrites; Allende (CV3), Murchison (CM2) and Tagish Lake (C2-ung). Finally, we discuss the origin of planetary scale Sr isotope heterogeneity.

Experimental: Conventional high-pressure acid digestion with $HF+HNO_3$ is ineffective for dissolving acid resistant SiC completely. An exception for decomposing SiC is high-pressure acid digestion at 250°C using $HF+HNO_3+H_2SO_4$ [9]. Each meteorite sample (200–600 mg) was placed in a PTEF insert of a high-pressure digestion system (DAB-2, Berghof) with 30M HF, 16M HNO_3, and 96% H_2SO_4. The insert was placed in a stainless jacket and heated at 250°C for >24 h. After sample digestion, the insert was placed on a hot plate and heated at 150°C to evaporate $HF+HNO_3$. The resulting solution was transferred to a quartz glass beaker and dried at 350 °C to evaporate the remaining H_2SO_4. 1M HCl was added to dissolve the dried residue containing water-insoluble $SrSO_4$ and $BaSO_4$. The sample solution was loaded on a cation exchange resin to remove major elements and SO_4^{2-} ions. Subsequently, Sr and REEs were collected by eluting 6M HCl. Sr was further purified by Eichrom Sr spec resin.

High-precision Sr isotope analysis were performed using TIMS (Triton-*plus*, Thermo). The purified Sr was loaded onto a single outgassed W filament using a Ta_2O_5 activator slurry. The results were obtained by averaging 100–400 ratios (2σ rejection level = 4.55% of the data) obtained in the static multicollection mode using five Faraday cups. The Sr isotope ratios were corrected for mass fractionation by assuming $^{86}Sr/^{88}Sr$ = 0.1194. Because a long-term fluctuation in Sr isotope ratios was observed during the course of this study, we divided the analytical period into several campaigns. The 2SD of the $^{84}Sr/^{86}Sr$ ratio for NIST 987 in individual campaigns ranged 27–32 ppm. The $^{84}Sr/^{86}Sr$ ratios for chondrites are reported in $\mu^{84}Sr$ units that are 10^6 relative deviations from the value of the NIST 987 analyzed in the same campaign.

Results and Discussion: The performance of the new digestion technique was evaluated by dissolving 2 mg of synthesized SiC powder (1 μm) using the same procedure applied to meteorites. After digestion, the solution was cooled to room temperature and centrifuged. No materials remained at the bottom of the centrifuge tube, confirming the complete dissolution of SiC. The maximum abundance of presolar SiC was estimated to be 20 ppm in chondrites [10]. Therefore, the dissolution of 2 mg SiC is in accord with the complete decomposition of presolar SiC in 1 g of chondrite sample (containing 0.02 mg SiC) using this approach.

Fig. 1 shows $\mu^{84}Sr$ values for the three chondrites obtained by multiple sample dissolutions. The reproducibilities (2SD) for the three meteorites range 17–35 ppm, which are comparable to those of NIST 987. This reflects complete dissolution of acid resistant presolar SiC with extremely low $\mu^{84}Sr$ (–800,000 ppm [11]). The $\mu^{84}Sr$ values in the bulk chondrites were generally consistent with those reported previously [2]. The bulk Tagish Lake sample had a slightly lower $\mu^{84}Sr$ (+30 ppm) than that for the bulk Allende (+58 ppm) and Murchison (+52 ppm) samples, judging from the obtained 2SE values as uncertainties.

Fig. 2 shows a plot of $\mu^{84}Sr-\varepsilon^{54}Cr$ for various bulk meteorites and CAIs. The bulk $\mu^{84}Sr$ values obtained in this study were used for Allende, Murchison, and Tagish Lake, and the other values were taken from the literature summarized in [12]. In this figure, the CAIs, carbonaceous chondrites, and other noncarbonaceous meteorites are plotted separately and result in a global positive correlation. At a detailed level, each meteorite group has a certain variation in the $\mu^{84}Sr-\varepsilon^{54}Cr$ space exceeding the analytical uncertainties of the individual data. In particular, although an overall correlation within the carbonaceous chondrites is not obvious, the three chondrites examined in this study with the $\mu^{84}Sr$ data show a negative correlation. Notably, the isotopic dichotomy seen for the carbonaceous chondrites and noncarbonaceous meteorites is also observed in plots of $\varepsilon^{50}Ti-\varepsilon^{54}Cr$ and $\Delta^{17}O-\varepsilon^{54}Cr$ [13].

Here, we propose a new volatilization model that accounts for the planetary scale isotope heterogeneity observed for multiple elements. Assuming that the isotopic composition of CI chondrites reflects that of the solar system average, the excess $\mu^{84}Sr$ and $\varepsilon^{54}Cr$ signatures in CAIs can be interpreted as resulting from the addition of materials sublimated from high $\varepsilon^{54}Cr$ and $\mu^{84}Sr$ carriers via thermal processing to a gaseous reservoir with an average solar isotopic composition. The carrier of large positive $\varepsilon^{54}Cr$ is nanoscale Cr spinel grains, while that for large $\mu^{84}Sr$ would be supernova grains with excess p- or r-process nuclides. The existence of supernova grains with large $\mu^{84}Sr$ is not evident in chondrites because they are too small to detect via SIMS (<10 nm) [14]. Although Os coexisted in supernova grains, the normal Os isotope composition in CAIs [15] suggests that these Os atoms were released via the sublimation of the supernova grains remaining in the solid phase such that no Os isotope anomalies were created in the gaseous phase. Such a process would be possible if the thermal processing temperature was sufficiently high to sublimate silicate, graphite, and spinel grains (>1400 K), as well as Sr and Cr atoms, but below the point of Os condensation (~1800 K). A similar conclusion was made by to explain the decoupling of Mo and W isotopes in bulk meteorites [16]. If thermal processing is the case, sublimation of SiC grains may be unavoidable at temperatures >1400 K. However, the elevated $\mu^{84}Sr$ values observed for the CAIs imply that sublimated supernova grains were more predominant than SiC grains during thermal processing. As a result, the residue from thermal processing had $\mu^{84}Sr$ and $\varepsilon^{54}Cr$ values lower than the solar system average. With respect to the difference in the results for the carbonaceous and noncarbonaceous chondrites, because carbonaceous planetesimals likely accreted at a greater radial distance from the sun than that of noncarbonaceous planetesimals [13], it is rational that noncarbonaceous planetesimals accreted from materials that underwent significant thermal processing and thus had relatively low $\mu^{84}Sr$ and $\varepsilon^{54}Cr$ values.

On the other hand, the variations in the $\mu^{84}Sr−\varepsilon^{54}Cr$ diagram within the two meteorite groups (carbonaceous and noncarbonaceous) may suggest that secondary processes other than global thermal processing led to the positive $\mu^{84}Sr−\varepsilon^{54}Cr$ correlation. Incorporation of CAIs at varying proportions into any single component (e.g., CI chondrite) can be ruled out as the cause of the variation of carbonaceous chondrites (Fig. 2). Size sorting of dust grains that survived the global thermal processing is a possible scenario [8], although it conflicts with a homogeneous Os isotope distribution. Alternatively, local thermal processing is more likely

to cause additional selective destruction of presolar grains different than that caused by global thermal processing. Because chondrule is a primary constituent of carbonaceous chondrite, flash heating for chondrule formation may have led to the variation in the $\mu^{84}Sr$ and $\varepsilon^{54}Cr$ values for carbonaceous chondrites. Therefore, analyzing the isotope anomalies for multiple elements, including Sr, for individual chondrules from different chondrite groups is important. Overall, the global positive trend and variations within the individual meteorite groups in the $\mu^{84}Sr−\varepsilon^{54}Cr$ diagram cannot be created by a single nebular process, but suggest a complicated history for the dust grains in the protoplanetary disk.
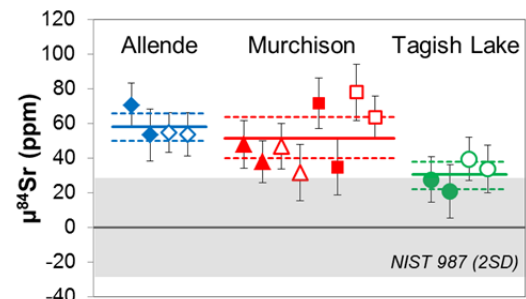
Fig. 1 *Repeated analyses of $\mu^{84}Sr$ for bulk chondrites. Same symbols are replicates of single sample dissolutions. Bold lines are average of individual meteorites, and dashed lines indicate 2SE of multiple isotopic runs.*
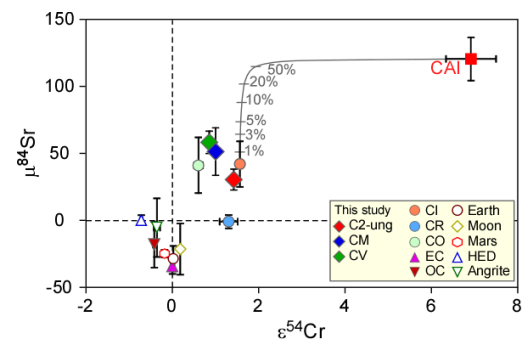
Fig. 2 *Plot of $\mu^{84}Sr$-$\varepsilon^{54}Cr$ for bulk meteorites and CAI.*

References: [1] Trinquier, A. et al. (2009) *Science 324*, 374. [2] Moynier, F. et al. *ApJ 758*, 45. [3] Burkhardt, C. et al. (2011) *EPSL 312*, 390. [4] Carlson, R. et al. (2007) *Science 316*, 1175. [5] Fehr, M. et al, (2005) *GCA 69*, 5351. [6] Sprung, P. et al. (2010) *EPSL 295*, 1. [7] Yokoyama, T. et al. (2010) *EPSL 291*, 48. [8] Dauphas, N. et al. (2010) *ApJ 720*, 1577. [9] Klemm, W. et al. (2001) *Fres J Anal Chem 370*, 641. [10] Nguyen, A. et al. (2011) *Elements 7*, 17. [11] Liu, N. et al. (2014) *LPSC 45*, 2049. [12] Yokoyama, T. et al. (2014) *EPSL in revision*. [13] Warren, P. (2011) *EPSL 311*, 93. [14] Kozasa, T. et al. (1991) *AA 249*, 474. [15] Yokoyama, T. et al. (2009) *LPSC 40*, 1489. [16] Burkhardt, C. et al. (2012) *EPSL 357*, 298.